SLAC-PUB-15501

BABAR Results on CP Violation in B Decays

Romulus Godang (On Behalf of the *BABAR* Collaboration)
Department of Physics, University of South Alabama, Mobile, Alabama 36688

We report on the study of the decay $B^+ \to D^0(\bar{D}0)K^+$ where D^0 and $\bar{D}0$ decaying to $K\pi\pi^0$, with the Atwood Dunietz and Soni (ADS) method. We measure the ratios Rads, R^+, R^- since the processes $B^+ \to D^0\bar{K}^+$ and $B^+ \to D^0K^+$ are proportional to V_{cb} and V_{ub}, respectively, are sensitive to r_B and to the weak phase γ.

1. Introduction

During recent years, several methods have been proposed to obtain the information on the Cabibbo-Kobayashi-Maskawa (CKM) [1, 2], phase angle γ. In the Standard Model (SM), the angle γ is the relative phase between $b \to c\bar{u}s$ and $b \to u\bar{c}s$ transitions as indicated in Fig. 1 and Fig. 2.

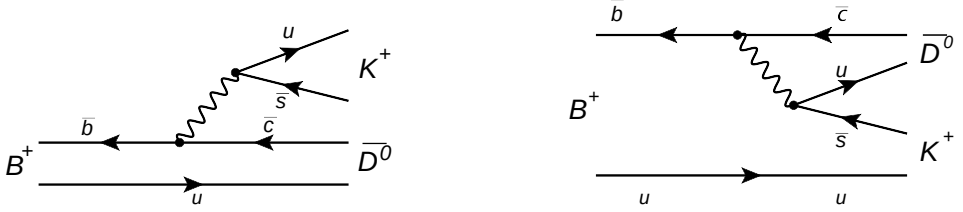

Figure 1: Feynman diagrams for $B^+ \to \bar{D}^0K^+$ ($b \to u\bar{c}s$))

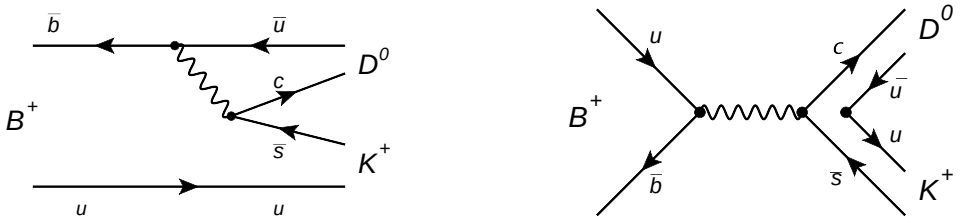

Figure 2: Feynman diagrams for $B^+ \to D^0K^+$ ($b \to c\bar{u}s$)

This phase angle γ can be measured using a variety of methods involving B-meson decays that mediated by either only tree-level or both tree-level and loop-level amplitudes. A theoretical source of information on the angle γ is provided by $B^- \to D^{(*)}K^-$ decays. The $D^{(*)}$ represents an admixture of $D^{(*)0}$ and $\bar{D}^{(*)0}$ states. These decays exploit the interference between $B^- \to D^{(*)0}K^-$ and $B^- \to \bar{D}^{(*)0}K^-$ that occurs when the $D^{(*)0}$ and $\bar{D}^{(*)0}$ decay to common final states.

In the Gronau-London-Wyler (GLW) method [3, 4], the D^0 meson is reconstructed based on Cabibbo-suppressed to CP-eigenstates, such as K^+K^-. In order to determine the angle γ from $B^\pm$ decays, we define the two experimental observables direct-CP-violating partial decay rate asymmetries as

$$A_{CP\pm} \equiv \frac{\Gamma(B^- \to D_{CP\pm}K^-) \ - \ \Gamma(B^+ \to D_{CP\pm}K^+)}{\Gamma(B^- \to D_{CP\pm}K^-) \ + \ \Gamma(B^+ \to D_{CP\pm}K^+)} = \frac{\pm 2r_B sin\delta_B sin\gamma}{1 + r_B^2 \pm 2r_B cos\delta_B cos\gamma} \tag{1}$$

We also define the two ratios of charged averaged partial rates using D meson decays to CP and flavor eigenstates as

$$R_{CP\pm} \equiv 2\frac{\Gamma(B^- \to D_{CP\pm}K^-) \ + \ \Gamma(B^+ \to D_{CP\pm}K^+)}{\Gamma(B^- \to D^0K^-) \ + \ \Gamma(B^+ \to \bar{D}^0K^+)} = 1 + r_B^2 \pm 2r_B cos\delta_B cos\gamma \tag{2}$$

Proceedings of the DPF-2011 Conference, Providence, RI, August 8-13, 2011

Work supported in part by US Department of Energy under contract DE-AC02-76SF00515.

SLAC National Accelerator Laboratory, Menlo Park, CA 94025

where $D_{CP\pm}$ refer to the CP eigenstates of D meson system and δ_B is the difference of their strong phases, and r_B is the magnitude of the ratio of the amplitudes for each decay

$$r_B \equiv \frac{|A(B^- \to \bar{D^0} K^-)|}{|A(B^- \to D^0 K^-)|} \tag{3}$$

In the Adwood-Dunietz-Soni (ADS) method [5, 6], the D^0 meson is reconstructed in the doubly Cabibbo-suppressed decay $D^0 \to K^+\pi^-$ from the favored $b \to c$, while the $\bar{D^0}$ meson from the favored $b \to u$ suppressed amplitude is reconstructed in the favored decay $\bar{D^0} \to K^+\pi^-$. By ignoring the possible effect due to the D meson mixing, we define the the charge ratio of B^+ and B^- decay rate to the ADS final states R^+ and R^-, respectively.

$$R^+ = \frac{\Gamma(B^+ \to [K^-\pi^+]K^+)}{\Gamma(B^+ \to [K^+\pi^-]K^+)} = r_B^2 + r_D^2 + 2r_B r_D k_D \; cos(\gamma + \delta_B + \delta_D) \tag{4}$$

and

$$R^- = \frac{\Gamma(B^- \to [K^+\pi^-]K^-)}{\Gamma(B^- \to [K^-\pi^+]K^-)} = r_B^2 + r_D^2 + 2r_B r_D k_D \; cos(\gamma - \delta_B + \delta_D) \tag{5}$$

where r_B and r_D are the suppressed to favored B and D amplitude ratios as

$$r_B \equiv \frac{|A(B^+ \to D^0 K^+)|}{|A(B^+ \to \bar{D^0} K^+))|} \tag{6}$$

and

$$r_D^2 = \frac{\Gamma(D^0 \to K^+\pi-)}{\Gamma(D^0 \to K^-\pi^+)} \tag{7}$$

and δ_B and δ_D are the strong phase differences between the two B and the two D, respectively.

2. *BABAR* Detector

The results presented in this paper are based on the entire $B\bar{B}$ data sample collected with the *BABAR* detector at the PEP-II asymmetric-energy B factory at the SLAC National Accelerator Laboratory. The $B\bar{B}$ pairs are produced from the decays of $\Upsilon(4S)$ resonance (on-resonance) that originate in collisions of 9.0 GeV electrons and 3.1 GeV positrons. The on-resonance data sample has a mean energy of 10.58 GeV and an energy rms spread of 4.6 MeV. The off-resonance (continuum) data sample has a center-of-mass (CM) energy 40 MeV below the resonance.

A detailed description of the *BABAR* detector and the algorithms used for track reconstruction and particle identification is provided elsewhere [7]. A brief summary is given here. High-momentum particles are reconstructed by matching hits in the silicon vertex tracker (SVT) with track elements in the drift chamber (DCH). Lower momentum tracks, which do not leave signals on many wires in the DCH due to the bending induced by a magnetic field, are reconstructed in the SVT alone. Electrons are identified by the ratio of the track momentum to the associated energy deposited in the calorimeter (EMC), the transverse profile of the shower, the energy loss in the drift chamber, and information from a Cherenkov detector (DIRC). The *BABAR* detector Monte Carlo simulation is based on GEANT4 [8]. We use EVTGEN [9] to model the kinematics of B meson decays and use JETSET [10] to model off-resonance process $e^+e^- \to q\overline{q}$ ($q = u$, d, s, or c quark).

3. Data Sample

In the GLW method [11], we use $(467\pm5)\times10^6$ $B\overline{B}$ pairs, approximately equally divided into $B^0\overline{B}^0$ and B^+B^-. The data have been collected in the years from 1999 until early 2008. We have reconstructed $B^\pm \to DK^\pm$ decays, with D mesons decaying to non-CP ($K\pi$), and CP-even ($K^+K^+, \pi^+\pi-$), and CP-odd ($K^0_s\pi^0, K^0_s\phi, K^0_s\omega$) eigenstates.

In the ADS method, we use two results where D^0 mesons are reconstructed into two modes, $D^0 \to K^+\pi^-$ [12] and $D^0 \to K^+\pi^-\pi^0$ [13], respectively. In $D^0 \to K^+\pi^-$ mode we use a data of $(467 \pm 5) \times 10^6$ $B\overline{B}$ pairs. We

present a search of the decays $B^- \to D^{(*)}K^-$, where the neutral D mesons decay into $K^+\pi^-$ final state (WS). In this paper, we first applied to $B^- \to D^{(*)}\pi^-$, where the neutral D mesons decay into the Cabibbo-favored $(K^-\pi^-)$ and doubly suppressed mode. In $D^0 \to K^+\pi^-\pi^0$, we use $(474 \pm 5) \times 10^6$ $B\overline{B}$ pairs. An additional off-resonance data sample of 45 fb^{-1} , collected at a center-of-mass energy 40 MeV below the $\Upsilon(4S)$ resonance, is used to study the $e^+e^- \to q\overline{q}$ background. In this paper, we studied the decays D^0 and $\bar{D}^0$ in which decays to $K^\mp\pi^\pm\pi^0$ final states.

4. Measurement of the CKM angle γ

4.1. CP Observables in $B^\pm \to D_{CP}K^\pm$ (GLW)

We identify signal $B \to DK$ and $B \to D\pi$ candidates using two defined kinematic variables. The first variable is the difference between the CM energy of the B meson (E_B^*) and the beam energy (ΔE) and the beam-energy-substituted mass (m_{ES}), respectively.

$$\Delta E = E_B^* - \sqrt{s}/2 \tag{8}$$

We estimate the irreducible background yields in our sample by exploiting the fact that the D invariant mass distribution fir this background is approximately uniform, while the signal event peaks around the nominal D mass.

Figure 3 shows the ΔE projections of the final fits to the CP subsamples. The curves are the full PDF (solid, blue) and $B \to D\pi$ (dash-dotted, green) stacked on the remaining backgrounds (dotted, purple). The region between the solid and the dash-dotted lines represents the contribution of $B \to DK$. Figure 4 shows m_{ES} projections as well as projections to the fit to the $D^0 \to K^-\pi^+$ flavor mode. The line definitions are the same as described in Fig. 3. We obtain the most precise measurements of the GLW parameters $A_{CP\pm}$ and $R_{CP\pm}$:

$$A_{CP+} = 0.25 \pm 0.06(stat) \pm 0.02(syst) \qquad A_{CP-} = -0.09 \pm 0.07(stat) \pm 0.02(syst) \tag{9}$$

$$R_{CP+} = 1.18 \pm 0.09(stat) \pm 0.05(syst) \qquad R_{CP-} = 1.07 \pm 0.08(stat) \pm 0.04(syst) \tag{10}$$

We measure a value of A_{CP+} which is 3.6 standard deviations from zero, which constitutes the first evidence for direct CP violation in $B \to DK$ decays.

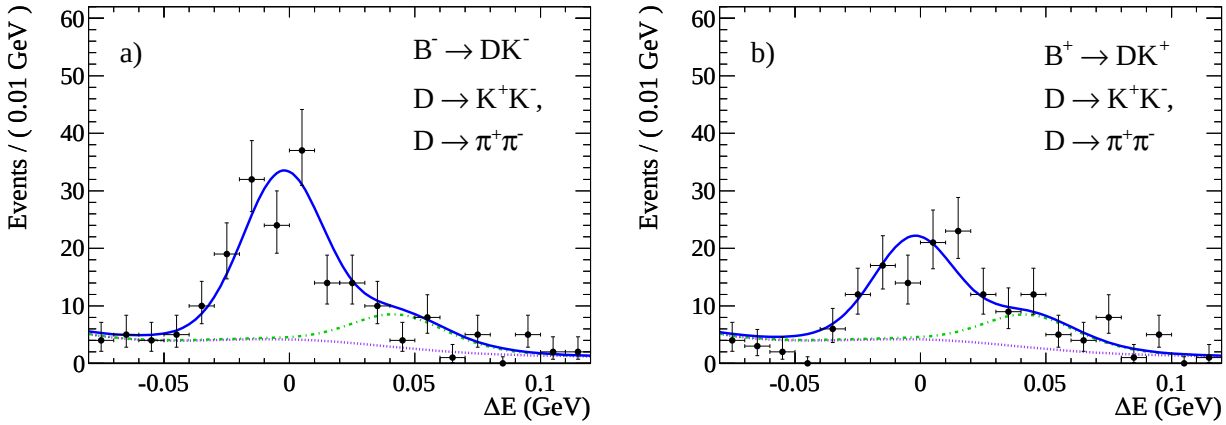

Figure 3: ΔE projections of the fits to the data, split into subset of define CP of the D candidate and charge of the B candidate: a) $B^- \to D_{CP+}K^-$ and b) $B^+ \to D_{CP+}K^+$

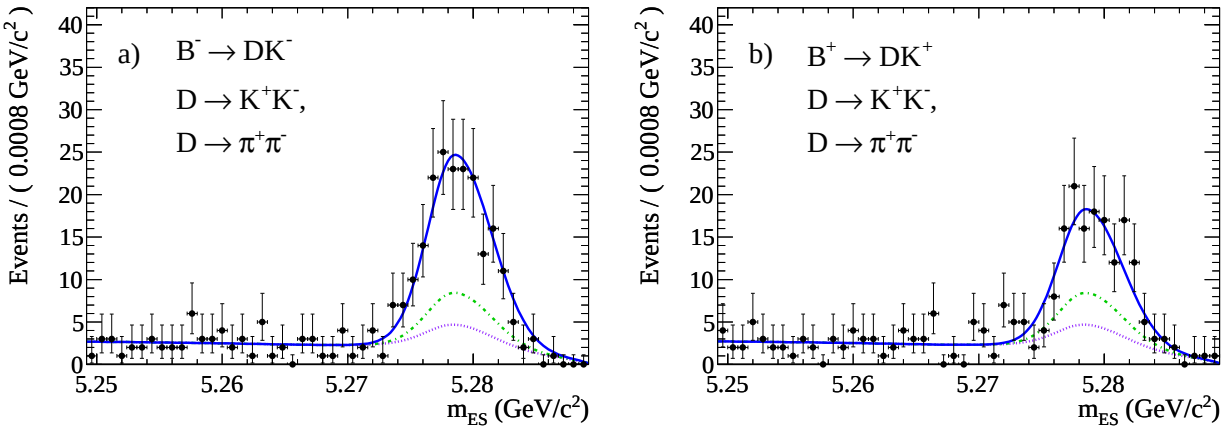

Figure 4: m_{ES} projections of the fits to the data, split into subset of define CP of the D candidate and charge of the B candidate: a) $B^- \to D_{CP+}K^-$ and b) $B^+ \to D_{CP+}K^+$

4.2. CP Observables in $B^- \to DK^-$ and $B^- \to D^*K^-$ (ADS)

We reconstruct $B^- \to D^{(*)}K^-$ and $B^- \to D^{(*)}\pi^-$ with the D meson decaying to $K^-\pi^+$ (RS = right-sign) and $K^+\pi^-$ (WS = wrong-sign). Charged conjugate reactions are assumed throughout this paper. For decays involving a D^*, both $D^* \to D\pi^0$ and $D^* \to D\gamma$ are reconstructed. To study the $B\overline{B}$ background for each signal category and charge combination (RS and WS) we use a sample of $e^+e^- \to \Upsilon(4S) \to B\overline{B}$ Monte Carlo events corresponding to about 3 times the data luminosity.

In this paper the off-resonance background events are reduced by using a multilayer perceptron artificial neural network with 2 hidden layers, available in the framework of TMVA package [14]. We use the neural network to select the discriminating variables.

Figure 5 shows the projections on m_{ES} and neural network (NN) of the fit results for DK^+ mode for samples enriched in signal with the requirements $NN > 0.94$ for m_{ES} projections or $5.2725 < m_{ES} < 5.2875\ GeV/c^2$. The point with error bars are data. The curves represent the fit projections for signal plus background (solid), the sum of all background components (dashed), and $q\overline{q}$ background only (dotted). The results of fits to the B^+ and B^- sample

$$R^+ = (2.2 \pm 0.9 \pm 0.3) \times 10^{-2} \qquad R^- = (0.2 \pm 0.6 \pm 0.2) \times 10^{-2} \tag{11}$$

and we extracted the variables $r_B^{(*)}$

$$r_B = (9.5^{+5.1}_{-4.1})\% \qquad r_B^* = (9.6^{+3.5}_{-5.1})\% \tag{12}$$

4.3. CP Observables in $B^\pm \to [K^\mp\pi^\pm\pi^0]K^\pm$ (ADS)

In this paper the off-resonance background events, in contrast to $B\overline{B}$ events, are characterized by a jet-like topology. We use a Fisher discriminant $\mathcal{F}$ to discriminate between the two categories of events. The Fisher discriminant is a linear combination of six variables. We choose the coefficients of the linear combination to maximize the separation between the signal and the off-resonance background. For the signal the Fisher discriminant $\mathcal{F}$ peaks at 1 and -1 for the off-resonance events. Since the correlations among the variables are negligible, we write the PDFs as products of one dimensional distributions of the m_{ES} and $\mathcal{F}$. We use MC samples to check the absence of the correlation between these distributions.

The PDF parameters are derived from data sample when possible in order to reduce the systematic uncertainties. The parameters for the continuum events are determined from the off-resonance data sample. We use the data sample of $B^+ \to D\pi^+$ with $D \to K^+\pi^-\pi^0$ to extract the parameters for the m_{ES} distribution. The parameters for the non-peaking $B\overline{B}$ distributions and the signal Fisher PDF are determined from the MC sample.

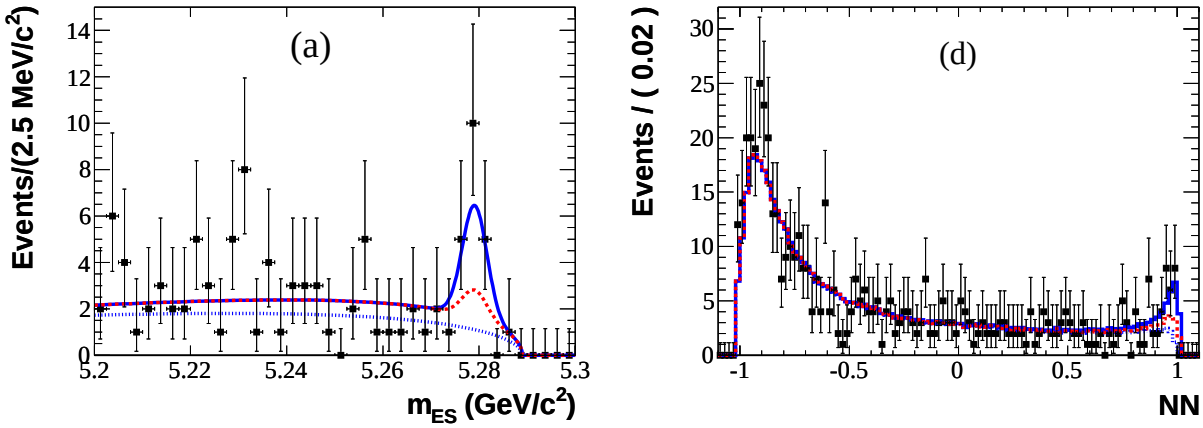

Figure 5: Projections on m_{ES} and neural network (NN) of the fit results for DK^+ mode for samples

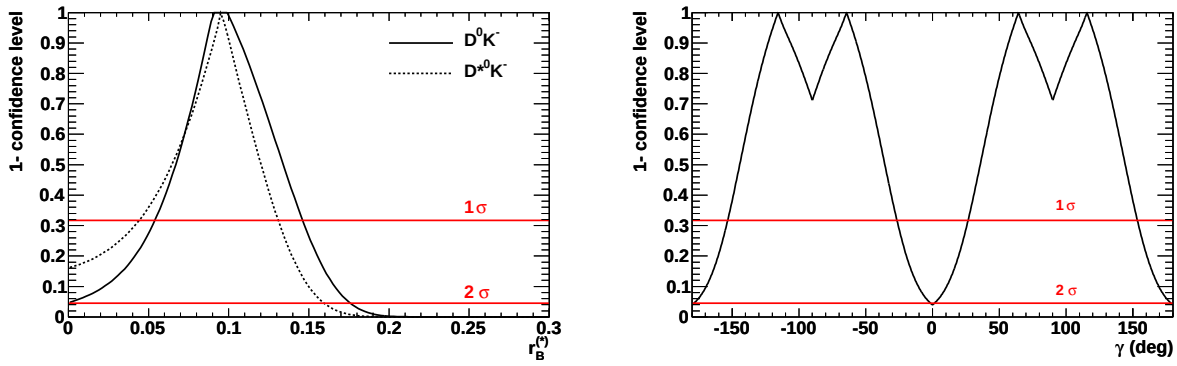

Figure 6: Constraints on $r_B^{(*)}$ from combined $B^- \to [K\pi]K^-$ ADS measurements (left) and constraints on angle γ from combined $B^- \to D^{(*)}[K^+\pi^-]K^-$ ADS measurements (right).

The fits to the m_{ES} for $\mathcal{F} > 0.5$ and the Fisher discriminant $\mathcal{F}$ distribution with $m_{ES} > 5.27$ GeV/c^2 for the combined B^+ and B^- samples are shown in Fig. 7 and Fig. 8, respectively. The data are well described by the overall fit results (solid blue line) which is the sum of the signal, continuum background, non-peaking $B\overline{B}$ background, and peaking $B\overline{B}$ background. We have presented a study of the decays $B^\pm \to D^0 K^\pm$ and

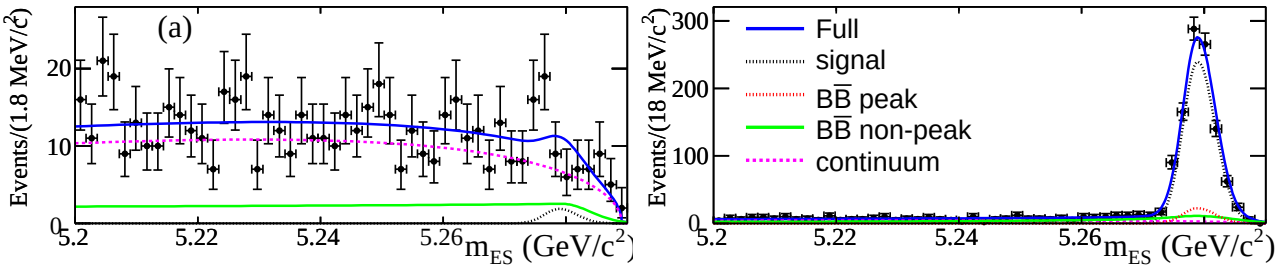

Figure 7: Distribution of m_{ES} (a,b) with $\mathcal{F} > 0.5$.

$B^\pm \to \bar{D}^0 K^\pm$, in which the D^0 and $\bar{D}^0$ mesons decay to $K^\pm\pi^\pm\pi^0$ final state using the ADS method. The final results are

$$R^+ = (5^{+12+1}_{-10-4}) \times 10^{-3} \qquad R^- = (12^{+12+2}_{-10-4}) \times 10^{-3} \tag{13}$$

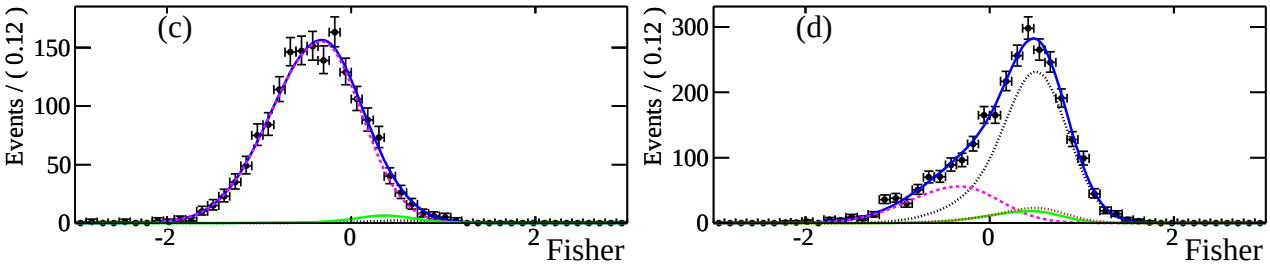

Figure 8: Distribution of $\mathcal{F}$ (c,d) with $m_{ES} > 5.27$ GeV/c^2.

from which we obtain 90% probability limits

$$R^+ < 23 \times 10^{-3} \qquad\qquad R^- < 29 \times 10^{-3} \tag{14}$$

Following a Bayesian approach [15, 16], the probability distributions for the R^+ and R^- ratio obtained in the fit are translated into a probability distribution for r_B. Figure 9 shows the posterior probability distribution. Since

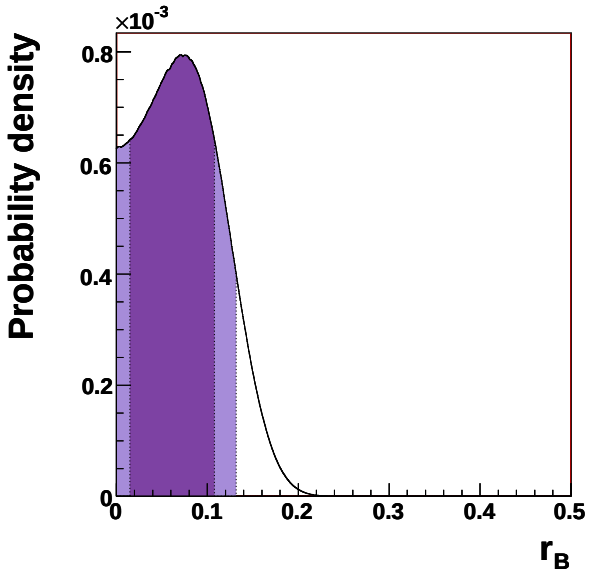

Figure 9: Bayesian posterior probability density function for r_B from our measurement of R^+ and R^- and the hadronic D decay parameters r_D, δ_D, and k_D.

the measurements are not statistically significant, we integrate over the positive portion of that distribution and obtain the upper limit $r_B < 0.13$ at 90% probability, and the range

$$r_B \in [0.01, 0.11] \tag{15}$$

at 68% probability and 0.078 as the most probable value.

Acknowledgments

The author would like to thank the organizers of DPF 2011 for their excellent program and kind hospitality. The supports from the *BABAR* Collaboration, the University of South Alabama, and the University of Mississippi are gratefully acknowledged. This work was supported by the U.S. Department of Energy under grant No. DE-FG02-96ER-40970.

References

1 N. Cabibbo, Phys. Rev. Lett. **10**, 531 (1963).
2 M. Kobayashi and T. Maskawa, Prog. Theo. Phys. **49**, 652 (1973).
3 M. Gronau and D. Wyler, Phys. Lett. **B265**, 172 (1991).
4 M. Gronau and D. London, Phys. Lett. **253**, 483 (1991).
5 D. Adwood, I. Dunietz, and A. Soni, Phys. Rev. Lett. **78**, 3257 (1997).
6 D. Adwood, I. Dunietz, and A. Soni, Phys. Rev. D **63**, 036005 (2001).
7 B. Aubert *et al.*, *BABAR* Collaboration, Nucl. Instr. Methods Phys. Res., Sect. A **479**, 1 (2002).
8 S. Agostinelli *et al.*, GEANT4 Collaboration, Nucl. Instr. Methods Phys. Res., Sect. A **506**, 250 (2003).
9 D. Lange, Nucl. Instr. Methods Phys. Res., Sect. A **462**, 152 (2001).
10 T. Sjostrand, Comput. Phys. Commun. **82**, 74 (1994).
11 P. del Amo Sanchez *et al.*, *BABAR* Collaboration, Phys. Rev. D **82**, 072004 (2010).
12 P. del Amo Sanchez *et al.*, *BABAR* Collaboration, Phys. Rev. D **82**, 072006 (2010).
13 J. P. Lees *et al.*, *BABAR* Collaboration, Phys. Rev. D **84**, 012002 (2011).
14 A. Hoeker *et al.*, (TMVA Group), CERN Report No. CERN-OPEN-2007-007 (2007).
15 G. D'Agostini, CERN Report No. 99-03 (2003).
16 G. D'Agostini and M. Raso, arXiv:hep-ex/0002056 (2000).